Toward ocean attenuation tomography: Determining acoustic volume attenuation coefficients in seawater using eigenray amplitudes

J. D. Tippmann, J. Sarkar, C. M. A. Verlinden, W. S. Hodgkiss, and W. A. Kuperman

Citation: The Journal of the Acoustical Society of America **140**, EL247 (2016); doi: 10.1121/1.4962348
View online: https://doi.org/10.1121/1.4962348
View Table of Contents: https://asa.scitation.org/toc/jas/140/3
Published by the Acoustical Society of America

Toward ocean attenuation tomography: Determining acoustic volume attenuation coefficients in seawater using eigenray amplitudes

J. D. Tippmann,[a] J. Sarkar, C. M. A. Verlinden, W. S. Hodgkiss, and W. A. Kuperman
Scripps Institution of Oceanography, University of California, San Diego, 9500 Gilman Drive, La Jolla California 92093-0238, USA
jtippman@ucsd.edu, bsarkar@ucsd.edu, cmverlin@ucsd.edu, whodgkiss@ucsd.edu, wkuperman@ucsd.edu

Abstract: A deep-water experiment in the Pacific made *in situ* measurements of the volume attenuation coefficients of sea water in the mid-frequency range. The frequency, temperature, salinity, *p*H, and pressure dependent seawater attenuation coefficients were determined using a vertical line array that received and identified over 2000 unique paths from 1200 mid-frequency 3–9 kHz LFM source transmissions at a convergence zone range and depth up to 400 m. The results show no change in attenuation coefficients in this band compared to estimates from 30-year-old models previously determined from a combination of long-range ocean acoustic and laboratory experiments. The inversion also explores the feasibility of ocean acoustic attenuation tomography to further separate the depth-dependent chemical components responsible for the total attenuation loss through by isolating a group of deep-water refracting acoustic paths.

[GBD]
Date Received: March 1, 2016 **Date Accepted:** July 19, 2016

1. Introduction

Jin and Worcester[1] and, more recently, Duda[2] suggest that it is possible to determine a depth-dependent ocean property such as ocean acidity through the link with the seawater attenuation coefficient. Ocean properties such as temperature, salinity, *p*H, and pressure are known to impact attenuation differently in certain frequency bands,[3] a result of chemical relaxation effects.[4] Within the last decade there has been a significant interest in measuring ocean *p*H due to anthropogenic emissions causing ocean acidification and whether it will increase the ocean noise levels significantly.[5–7] Regardless of ocean acidification's affect on ocean noise, measuring ocean acidity is important for understanding the global carbon cycle.[8] Additionally, measuring attenuation over long-range transmissions can provide more insight into large-scale ocean acidity levels than from point measurements. Attenuation-based tomography brings the capability to measure depth-dependent ocean acidity not available through time of flight tomography, in addition to the other depth-dependent ocean variables, salinity and temperature, thereby enhancing the accuracy of propagation modeling.

Here, an experiment was conducted in the Northeast Pacific to measure the attenuation coefficients of sound in seawater *in situ* and to further explore the potential for attenuation tomography by identifying individual eigenray transmissions. The experiment involved acquiring underwater acoustic data with a known active source in the mid-frequency band (3 to 9 kHz) and then comparing the results to attenuation coefficients produced from equations established by Francois and Garrison,[4] and simplified by Ainslie and McColm.[9] Received acoustic levels from multiple acoustic ray paths for a given source transmission were measured at a range of one convergence zone (approximately 50 km) with a high resolution, 127-element vertical line array (VLA). At this range for sources between 3 and 9 kHz, the predicted total attenuation loss is approximately 7–38 dB, respectively. An ocean average attenuation at one convergence zone was estimated for each frequency in this band by using a least-squares solution to a system of linear equations. Attenuation coefficients for a group of very similar ray paths were also estimated.

---

[a]Author to whom correspondence should be addressed.

2. Experimental setup

The experiment was conducted in deep water located off the coast of Oregon, USA, where the depth was approximately 2820 m. A representative sound-speed profile [Fig. 1(a)] has an upper sound channel near the surface in addition to the standard deep water sound-speed profile.[10] The Scripps Institution of Oceongraphy's *R/V Melville* deployed a drifting VLA neutrally buoyant at approximately 300 m depth and then deployed a source approximately 50 km away from the VLA and within the first convergence zone. The source and receiver locations are shown in Fig. 1(b). For the data analyzed in this paper, the source emitted 2 s, 3–9 kHz linear frequency modulated (LFM) chirps continuously as it was lowered from the surface to a depth of 400 m at a rate of 11 m per minute over a duration of 37 min. The source was then maintained at a constant depth of 400 m for over 10 min.

The acoustic data were recorded at a sampling rate of 25 kHz on a 127-element VLA with 10 cm element spacing ($\lambda/2$ at 7.5 kHz). The dense sampling of the array and pulse compression of the received signals allowed for high resolution eigenray detection of multiple rays per source event. The array provided a beamwidth of approximately 1°.

3. Ray identification and transmission loss

A set of approximate eigenrays between the source and receiver were produced by matching a BELLHOP[11] propagation simulation ray to the experimental received angle of arrival and time of arrival for each individual ray by adjusting the range. An example set of eigenrays for one source event are shown as three highlighted eigenrays in Fig. 1(a). The eigenrays matched between simulation and experiment are shown in the background in Fig. 1(a) and represent the sampled region of the ocean waveguide during the entire source deployment.

The accumulation of all the best fits between the simulation and data are shown in Fig. 2 where simulation and experimentally observed rays are plotted as points in received angle versus time of arrival.

The experimental transmission loss (TL) of each ray was then determined from the subtraction of the power-spectral density (PSD) of the pulse-compressed signal received level (RL) from the calibrated source level (SL) at each frequency, as simply expressed in Eq. (1):

$$TL = SL - RL. \tag{1}$$

The source levels were determined through short-range source-array calibration transmissions. Because a roll off near 3 and 9 kHz in the source level resulted in larger errors towards the boundary of the LFM bandwidth, only spectral levels between 3.5 and 8.5 kHz were used.

The transmission loss at each frequency of each identified ray is a combination of geometric spreading loss [GL(b) where b is for each ray] and the frequency-dependent attenuation loss [AL(b,f)] as expressed in Eq. (2):

$$TL(b,f) = GL(b) + AL(b,f). \tag{2}$$

The geometric spreading loss for the observed rays sampled was estimated from a parabolic equation propagation simulation. Perturbations in the sound speed profile, however, cause scintillation that vary the observed levels around the mean geometric spreading loss, as discussed by Jin and Worcester[1] and Duda.[2] This was

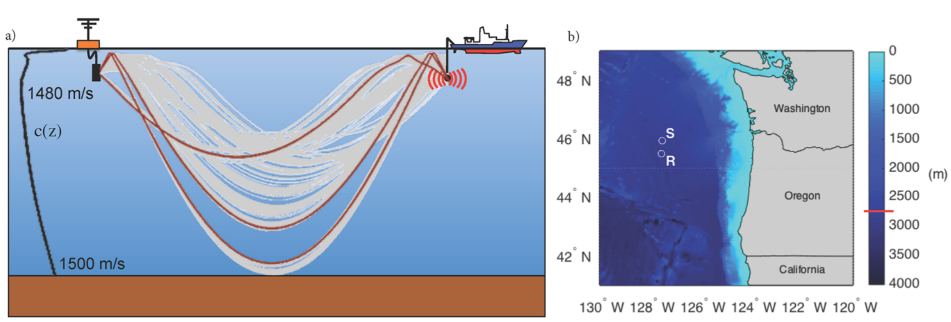

Fig. 1. (Color online) (a) The illustration shows the experimental setup with the source and receiver located in deep water. A representative sound-speed profile is plotted for reference. The light shaded eigenrays represent the regions sampled during the source deployment. The dark set of three eigenrays represent paths unique to one source position at 400 m depth. (b) Locations of the source (S) and receiver (R) in deep water (2820 m marked in red on the colorbar) located off the coast of Oregon, USA.

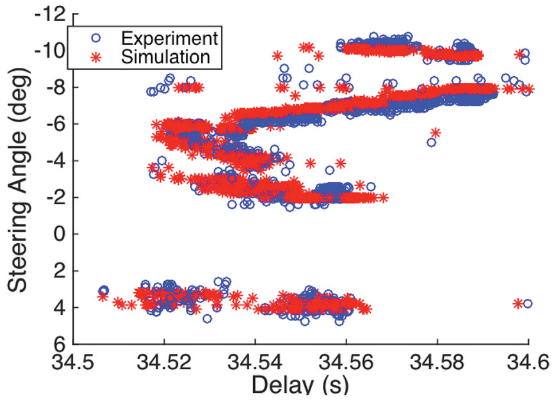

Fig. 2. (Color online) The arrival time of each ray is plotted against its beam steering angle (negative angle are upward looking beams) for both the experiment and the simulation. The experimentally observed rays include only those that were within 0.5° in angle and 0.01 s in time of a simulation ray for a given depth and range. Over 1800 rays were matched.

clearly evident in the TL data, demonstrating the requirement for treating the observed levels as a statistical distribution from multiple measurements rather than a single measurement.

4. Inverting for attenuation coefficients

We used the experimental TL observations matched to the simulations to solve for the attenuation through a least-squares solution to a system of linear equations. The attenuation loss component in Eq. (2) can be expanded as the product of a frequency-dependent sound absorption coefficient $\alpha(f)$ and ray path length $s(b)$, resulting in a TL expression in Eq. (3) that can be solved for $\alpha(f)$ and geometric loss $GL(b)$:

$$TL(b,f) = GL(b) + s(b) \cdot \alpha(f). \quad (3)$$

The unknowns can be further expanded as perturbations about mean values [Eq. (4)]. Expected values of the GL and AL are taken from the simulation TL estimates and the attenuation equation estimates, respectively,

$$TL(b,f) = (E[\bar{G}L] + \Delta GL(b)) + s(b) \cdot (E[\bar{\alpha}(f)] + \Delta\alpha(f)). \quad (4)$$

The resulting least-squares estimates of the frequency-dependent attenuation coefficient, shown in Fig. 3 as the thick solid lines with error bars for of an average of all ray groups and of a group of very similar ray paths, are compared to both the Thorp[12] equations (dashed) and the ray-integrated average using the Ainslie and McColm simplified version of the Francois and Garrison equation[4,9] (thin solid line). The error bars represent the combination of two errors: (1) the error of the least squares fit and (2) the error in the source level from the source-array calibration transmissions.

The group of very similar paths occurred when the source was stationary at a constant depth for 10 min. The two results are different in that one shows an average frequency dependent ocean attenuation estimate for the ocean highlighted by all gray ray paths in Fig. 1(a) and the other shows the attenuation estimate along of the ray paths shown in red in Fig. 1(a).

From the 1934 TL observations, only 327 independent observations exist assuming a correlation time of 30 s. The correlation time of 30 s was a worst case estimate calculated from the temporal auto-correlation of the TL for a group of very similar rays. When considering 410 transmission loss observations from a group of very similar rays, only 37 independent measurements exist using the same correlation time of 30 s.

5. Discussion and conclusion

The frequency-dependent attenuation coefficients found here from experimental data agree well with those calculated using Francois and Garrison,[13] showing the attenuation coefficients in the 3.5–8.5 kHz band have not changed over the past 30 years. More important than agreeing with a model based on data more than 40 years old is the result that climate related ocean change in the same time did not result in a significant change of the equations in this frequency range. It is important to note that this agreement is only in the region of the Northeast Pacific. Future experiments will focus on additional sites in the Pacific and Atlantic, where attenuation is often assumed to be higher than the Pacific.

Furthermore, these results show that *in situ* broadband measurements of attenuation in the mid-frequency range are possible with this experimental arrangement.

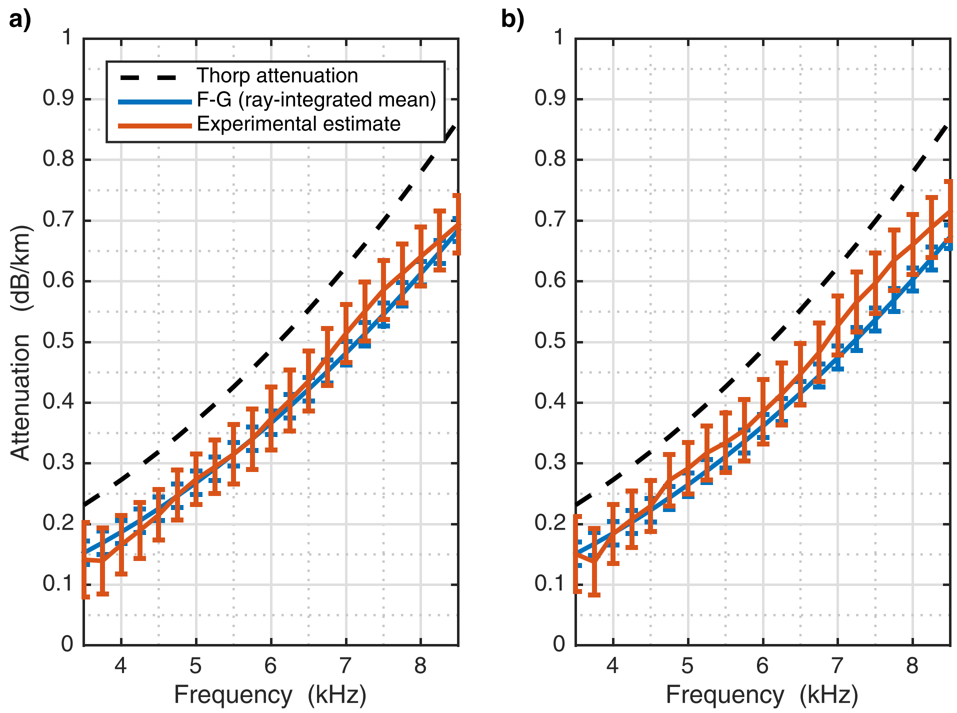

Fig. 3. (Color online) Experimental estimates with error bars of the frequency-dependent attenuation constant $\alpha(f)$ for 28 frequencies between 3.5 and 8.5 kHz are plotted against the empirical equation estimates developed by Thorp (Ref. 12) and Francois and Garrison (Ref. 4) for the two cases: (a) when all rays are included and (b) when only a group of very similar rays is included. The FG estimate for all rays is an average of all rays integrated through the experimental environmental profiles, where the FG estimate a for group of very similar rays is integration of only those rays.

The results demonstrate the challenge in having enough independent observations to reduce the error on the estimate of the attenuation as discussed by Duda.[2] Understanding the fluctuations further for reducing the error on the attenuation coefficients is critical for future work to estimate ocean properties such as *p*H.

Acknowledgments

The authors would like to acknowledge Bruce Cornuelle, Andrew Dickson, and Dave Ensberg at the Scripps Institution of Oceanography (SIO) for their guidance and time for very useful discussions on this work. This research was supported by the ONR.

References and links

[1]G. Jin and P. F. Worcester, "The feasibility of measuring ocean *p*H by long-range acoustics," J. Geophys. Res. **94**(C4), 4749–4756, doi:10.1029/JC094iC04p04749 (1989).
[2]T. F. Duda, "Revisiting experimental methods for studies of acidity-dependent ocean sound absorption," J. Acoust. Soc. Res. **125**(4), 1971–1981 (2009).
[3]M. Ainslie. *Principles of Sonar Performance Modelling, Springer Praxis Books in Geophysical Sciences* (Springer-Verlag, Berlin, 2010).
[4]R. E. Francois and G. R. Garrison, "Sound absorption based on ocean measurements. Part II: Boric acid contribution and equation for total absorption of sound," J. Acoust. Soc. Am. **72**(6), 1879–1890 (1982).
[5]Peter G. Brewer, "Ocean chemistry of the fossil fuel CO_2 signal: The haline signal of 'business as usual,' " Geophys. Res. Lett. **24**(11), 1367–1369, doi:10.1029/97GL01179 (1997).
[6]Keith C. Hester, Edward T. Peltzer, William J. Kirkwood, and Peter G. Brewer, "Unanticipated consequences of ocean acidification: A noisier ocean at lower pH," Geophys. Res. Lett. **35**(19), L19601, doi:10.1029/2008GL034913 (2008).
[7]D. Benjamin Reeder and Ching-Sang Chiu, "Ocean acidification and its impact on ocean noise: Phenomenology and analysis," J. Acoust. Soc. Am. **128**(3), EL137–EL143 (2010).
[8]Scott C. Doney, Victoria J. Fabry, Richard A. Feely, and Joan A. Kleypas, "Ocean acidification: The other CO_2 problem," Ann. Rev. Marine Sci. **1**(1), 169–192 (2009).
[9]M. A. Ainslie and J. G. McColm, "A simplified formula for viscous and chemical absorption in sea water," J. Acoust. Soc. Am. **103**(3), 1671 (1998).
[10]M. B. Porter, H. Schmidt, F. B. Jensen, and W. A. Kuperman, *Computational Ocean Acoustics* (AIP, Woodbury, NY, 2011).
[11]M. B. Porter, "The BELLHOP manual and user's guide: Preliminary draft" (January, 2011).
[12]W. H. Thorp, "Deep-ocean sound attenuation in the sub- and low-kilocycle-per-second region," J. Acoust. Soc. Am. **38**, 648–674 (1965).
[13]R. E. Francois and G. R. Garrison, "Sound absorption based on ocean measurements: Part I: Pure water and magnesium sulfate contributions," J. Acoust. Soc. Am. **72**(3), 896–907 (1982).